sented the Stokes parameters as a formal way to follow polarized radiation through the radiative transfer equation.

REFERENCES

For further reading

A thorough article that includes polarization fundamentals for atmospheres:

- Hansen, J. E., and Travis, L. D., 1974. "Light Scattering in Planetary Atmospheres." Space Sci. Rev. 16, 527–610.

A fundamental textbook that includes polarization:

- van de Hulst, H. C. 1981. *Light Scattering by Small Particles* (New York: Dover).

References for this chapter

1. Hansen, J. E., and Travis, L. D., 1974. "Light Scattering in Planetary Atmospheres." Space Sci. Rev. 16, 527–610.
2. van de Hulst, H. C. 1981. *Light Scattering by Small Particles* (New York: Dover).
3. Chandrasekhar, S. 1950. *Radiative Transfer* (Oxford: Oxford University Press).
4. Code, A. D., and Whitney, B. 1995. "Polarization from Scattering in Rhodes." Astrophys. J. 441, 400–407.
5. Seager, S., Whitney, B., and Sasselov D. D. 2000. "Photometric Light Curves and Polarization of Close-In Extrasolar Giant Planets." Astrophys. J. 540, 504–520.
6. Hansen, J. E., and Hovenier, J. W. 1974. "Interpretation of the Polarization of Venus." J. Atm. Sciences 31, 1137–1160.

Chapter Eight

Opacities

8.1 INTRODUCTION

The way in which radiation moves through a planet atmosphere is controlled by opacities: the numbers of molecules, atoms, or condensates present and their absorbing characteristics. By absorbing and emitting stellar radiation, the gas and solid opacities have deep consequences for so many of the physical characteristics of the atmosphere (see Figure 8.1). The planet atmosphere temperature structure depends on where and how much of the incoming and outgoing radiation is absorbed, scattered, and thermally reradiated. Whether or not convection occurs depends in part on the magnitude of opacities; if radiative energy transport is impeded by the opacities, then energy transport by convection will set in. The planetary spectrum arises from absorption and emission of radiation. Most significantly for physical characterization of exoplanets, the planetary spectrum is one of the most important observables.

In this chapter we address the fundamentals of opacities: molecular energy levels and their populations, and absorption cross sections. We focus on molecules and not atoms. Due to planetary temperatures, molecules dominate observable exoplanetary spectra. We aim to understand why the absorption bands of an individual molecule are located at a given frequency and with a given line strength. We also strive for a basic picture of absorption and scattering from solid particles. Condensates—solid particles congregating as clouds or haze layers—can have strong opacities and are expected to form in many planetary atmospheres.

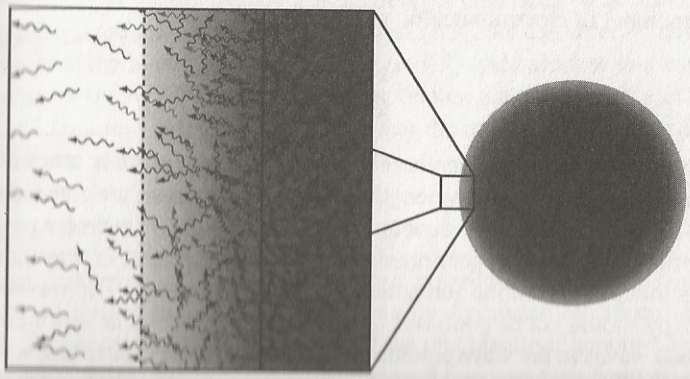

Figure 8.1. Illustration of photons emerging from a giant planet atmosphere. Based on [1].

As an introduction to opacities we review the expression for the absorption coefficient α (equation [5.9] from Section 5.2.4),

$$\alpha(T, P, \nu) = \sum_j \sum_i n_{ji}(T, P)\sigma_{ji}(T, P, \nu). \tag{8.1}$$

The absorption coefficient is made up of contributions from each gas species j. In Chapter 4 we described chemical equilibrium, nonequilibrium, and photochemistry calculations that led to the number densities (in units of m^{-3}) of different molecules. For each kind of molecule j, there are contributions from molecules with different energy states i. More specifically, the term n_{ji} refers to the number density of molecules j in energy state i. The number density of molecules is determined by chemical reactions at the ambient temperature and pressure in a specific atmosphere layer (Section 4.3) and by cloud processes (Section 4.4).

The focus of the first part of this chapter is on the energy levels and absorption cross sections for transitions between energy levels. In the second part, we turn to describe the emission coefficient, with a focus on scattering from condensates.

8.2 ENERGY LEVELS IN ATOMS AND MOLECULES

Atoms and molecules have many individual energy levels that are characteristic of the specific atom and molecule. From quantum mechanics, we know that atoms and molecules have discrete energy states, unlike classical particles which can have any energy. The difference between two energy levels corresponds to the wavelength of spectral features via the relation $\Delta E = h\nu$, where h is Planck's constant and E is the amount of energy absorbed by or carried away from an atom or molecule by a photon.

For planetary atmospheres we are interested in the emergent spectrum. Planetary scientists use wavelength, frequency, or wavenumber to describe the energy of spectral features, and not the energy of the atomic or molecular transition itself. The wavenumber of electromagnetic radiation is defined as

$$\tilde{\nu} = \frac{1}{\lambda} = \frac{\nu}{c} = \frac{E}{hc} \tag{8.2}$$

in units of m^{-1} or more conventionally cm^{-1}. Wavenumber is more often used among spectroscopists than wavelength because energy levels are conveniently proportional to wavenumber (or frequency) but inconveniently inversely proportional to wavelength. Similarly, spectrometers are often calibrated in wavenumber because it is independent of the fundamental constants c and h. The wavenumber in spectroscopy should not be confused with the angular or circular wavenumber used to described waves in the wave equation. When describing a spectrum, wavelength, frequency, and wavenumber are often used interchangeably. We will either use $\tilde{\nu}$ to denote wavenumber, or make it clear whenever ν refers to wavenumber.

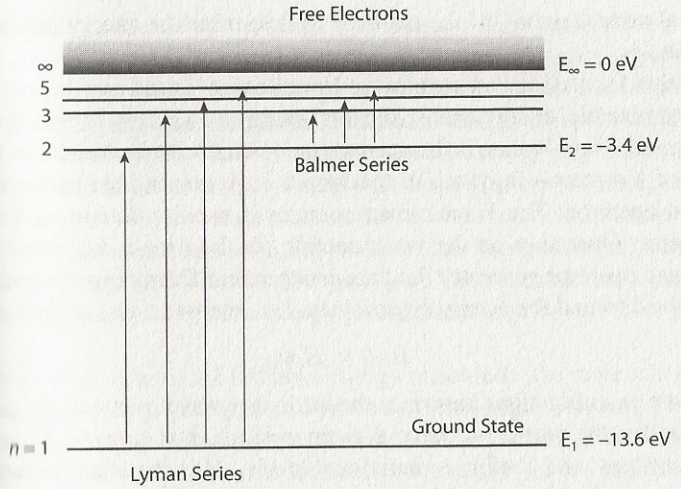

Figure 8.2 Hydrogen energy level diagram. See equation [8.3].

8.2.1 Atoms

Let us start with the Bohr model of the hydrogen atom as a way to recall some of the basics of atomic energy levels. The Bohr model for an isolated atom is that of a postively charged nucleus with electrons orbiting in successive orbits. Bohr developed the basic picture that electrons in an atom have stationary states, or energy levels, and that when an electron changes its energy level a photon is emitted or absorbed. Bohr used the equation of motion of an electron, including the kinetic energy and Coulomb potential energy terms, to derive the total energy state of an atomic system:

$$E_n = -\frac{me^4}{8\epsilon_0^2 h^2}\frac{1}{n^2} = -\frac{R_H hc}{n^2}, \tag{8.3}$$

where $n = 1, 2, \ldots \infty$. Here m is the mass of the electron, e is the electron charge, ϵ_0 is the electric constant, and R_H is Rydberg's constant. n is now known as the principal quantum number. From equation [8.3], we can directly calculate the energy levels of the hydrogen atom (see Figure 8.2) and calculate the wavenumber or frequency of hydrogen energy transitions, that is, the wavenumber of hydrogen line spectral features. Bohr also postulated that the angular momentum L can take on only discrete values:

$$L = n\frac{h}{2\pi}. \tag{8.4}$$

Bohr reached his model and equations from experimental evidence and heuristic arguments, motivated by the desire to explain the hydrogen gas spectrum and frequencies. To proceed to atoms with more than one electron, quantum mechanical equations are needed. We will therefore review a few concepts from quantum mechanics. Although we will not solve any equations in this chapter, our aim is for a

conceptual understanding of the pathway to determine the energy levels of atoms and molecules.

Recall that for classical mechanics the Hamiltonian is used as a description of the kinetic and potential energy, that is, the total energy, of a closed system. In quantum mechanics, the Hamiltonian is the operator associated with the kinetic and potential energies of a system—in quantum mechanics each measurable parameter has an associated operator. The Hamiltonian operator is used to determine the energies of a system. Operating on the wavefunction, in the time-independent case, the Hamiltonian operator generates the time-independent Schrodinger equation which can be solved to find the energy eigenvalues (i.e., energy levels) of the system:

$$H\psi_i = E_i\psi_i, \tag{8.5}$$

where ψ are eigenfunctions known as the stationary wavefunctions, the probability amplitudes for the particle to have a given position x at time t. E_i are the energy eigenvalues, and i refers to individual levels. H is the Hamiltonian operator associated with the kinetic and the potential energy and in one dimension is

$$H = \frac{-\hbar^2}{2m}\frac{\partial^2}{\partial x^2} + V(x), \tag{8.6}$$

where x is position. Here we have taken the kinetic energy as $p^2/2m$ where p is momentum and m is mass. We have used $\frac{d^2\psi}{dx^2} = -\frac{p^2}{\hbar}\psi$ and considered wavefunctions of the form $\psi(x,t) = Ae^{i(kx-\omega t)}$. The 1D time-independent (nonrelativistic) Schrodinger equation is then

$$\boxed{\frac{-\hbar^2}{2m}\frac{d^2\psi(x)}{dx^2} + V(x)\psi(x) = E\psi(x).} \tag{8.7}$$

The energy levels of the hydrogen and other atoms can be derived from Schrodinger's equation by specifying $V(x)$, that is, how the potential energy changes with location. For the hydrogen atom, one can treat the potential energy term as a classical Coulomb potential,

$$V(r) = \frac{e^2}{4\pi\epsilon_0}\frac{1}{r}, \tag{8.8}$$

where r is the radial distance of the electron from the force center and in equation [8.7] r replaces x and m is the reduced mass of the system. For hydrogen and hydrogen-like ions, the energy levels can be computed analytically. For many electron atoms, the potential is more complicated and computers are needed to work out solutions to the Schrodinger equation.

8.2.2 Molecules

Conceptually, a molecule can be visualized as number of atoms bound together by a balance of mutually attractive and repulsive forces. Molecules undergo electronic transitions just as atoms do. In electronic transitions, the electron moves from a lower to a higher energy level upon absorption of a photon, and the molecule emits a photon as the electron drops to a lower energy level. An electronic transition typically involves a few eV ($\sim 10^4$ cm^{-1}) of energy. This transition energy corresponds to photons in the UV or visible range of the electromagnetic spectrum.

Molecules, unlike atoms, have energy transitions other than electronic transitions. These rotational and vibrational transitions lead to complex band systems. The molecule as a whole rotates about any spatial axis, giving rise to rotational transitions. The individual atoms vibrate with respect to one another, causing vibrational transitions. When vibrational motion occurs, rotational motion is always induced. The water vapor molecule, for example, has hundreds of millions of lines from combined rotational-vibrational transitions. The molecular spectral lines resulting from transitions between energy levels blend together to form molecular bands.

For rotational or vibrational radiative energy transitions, the molecule must couple with an electromagnetic field so that energy exchanges can take place. This coupling is generally provided by the electric dipole moment of the molecule. A dipole moment in a molecule exists if the effective centers of the positive and negative charges of the molecule have nonzero separation. Essentially, a molecule has a dipole moment if it has a difference between the center of charge and the center of mass. For example, H_2O and O_3 have permanent electric dipole moments due to their asymmetrical charge distributions. Linear molecules, such as N_2, O_2, and CO_2 are examples of molecules that have no permament dipole moment because of their symmetrical charge distributions,. Lack of a permanent dipole moment theoretically means the gas species has no rotational-vibrational transitions. Dipole moments can be temporarily induced. For example, asymmetric bending or stretching modes of vibration induce a dipole moment (e.g., CO_2). In addition, the weaker electric quadrupole or magnetic dipole moments may exist and cause vibrational transitions.

To get some perspective on energy levels in molecules we show a potential energy diagram for molecular transitions in Figure 8.3. Two stable electronic states of a diatomic molecule are shown. Each electronic state has several vibrational states of lower energy associated with it. Each vibrational state, in turn, has many even lower-energy rotational states associated with it.

To quantitatively describe molecular rotational and vibrational energy levels we will adopt a conventional, pedagogical, yet mechanical model of the molecule. This model ignores the detailed structure of the molecule in terms of nuclei and electrons, but enables us to get a handle on the origin and structure of molecular lines.

8.2.2.1 Molecular Rotational Transitions

We will begin with the pure rotational spectrum of a diatomic molecule. To gain a conceptual understanding of the origins of the rotational energy levels, we take the conventional approximation of a rotating diatomic molecule as a rigid rotor. In this picture, the atoms are the two masses with a fixed separation and rotating about an axis that goes through the common center of mass (Figure 8.4.) We are assuming that the diatomic molecule can rotate about the common center of mass without changing the separation or relative positions of the constituent atoms.

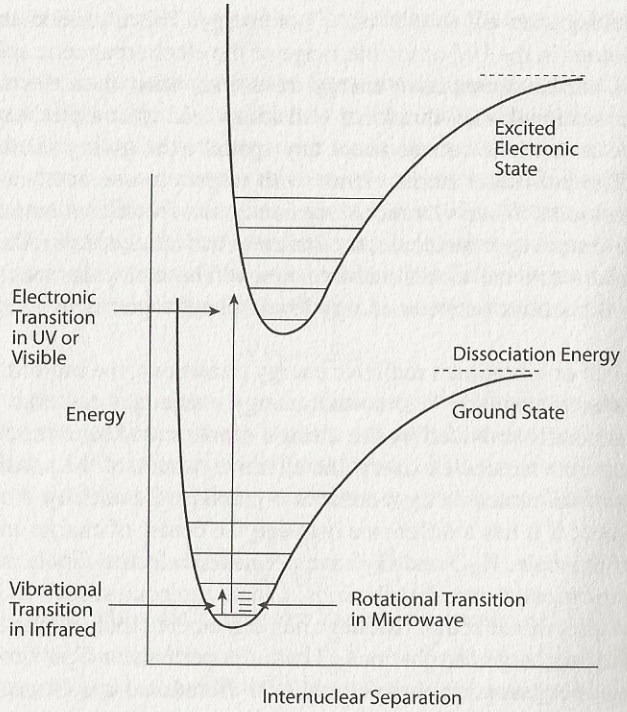

Figure 8.3 Schematic illustration of molecular electronic, vibrational, and rotational energy levels. Note that near the potential energy minimum of an electronic energy state, the potential energy curve can be approximated by a parabola in the same functional form as the simple harmonic oscillator potential. Adapted from [2].

Our aim is to understand where the rotational energy levels of a diatomic molecule come from. We will use the time-independent Schrodinger equation framework presented in Section 8.2.1, and find the eigenvalues for the 1D time-independent Schrodinger equation with the relevant kinetic and potential energy terms. In fact, a rigid rotor has no potential energy. We are literally making the assumption that the atoms in the diatomic molecule are completely fixed with respect to each other.

Classically, a rigid rotor with angular velocity ω has moment of inertia[1] I,

$$I = \sum_i m_i r_i^2 = m_1 r_1^2 + m_2 r_2^2, \tag{8.9}$$

where r_1 and r_2 are the distances of the atoms from the common center of mass. The angular momentum of a classical rigid rotor is

$$L = \sum_i m_i \omega r_i. \tag{8.10}$$

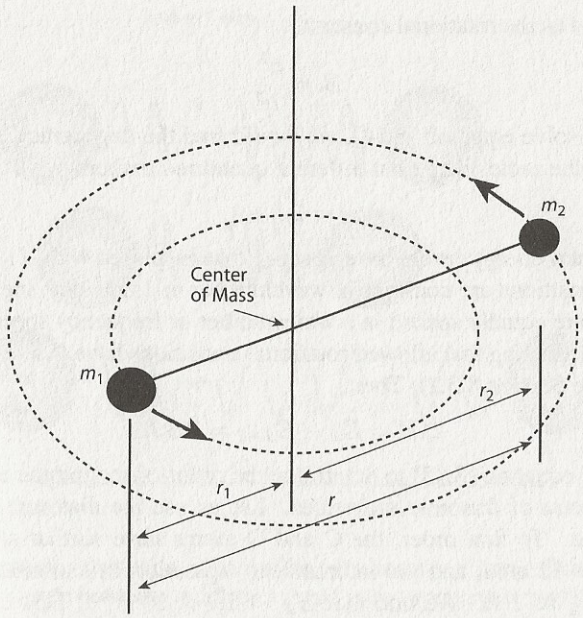

Figure 8.4 Schematic illustration of the rigid rotor. The rigid rotor is used as an approximate model for a diatomic molecule.

The classical rotational kinetic energy from a rigid rotor is therefore

$$E = I\omega^2 = \frac{L^2}{2I}. \tag{8.11}$$

We may now associate the classical rotational energy term with the quantum mechanical Hamiltonian operator,

$$H\psi = \frac{L^2}{2I}\psi = E_J\psi \tag{8.12}$$

or

$$L^2\psi = 2IE_J\psi. \tag{8.13}$$

The wavefunction solutions ψ to this equation are actually the spherical harmonics $Y_{l,m}(\theta, \phi)$. If we were to put the spherical harmonics into equation [8.13], then we would find

$$L^2 Y_{l,m}(\theta,\phi) = J(J+1)\hbar^2 Y_{l,m}(\theta,\phi) = 2IE_J\psi \tag{8.14}$$

or

$$\boxed{E_J = J(J+1)\frac{\hbar^2}{2I}} \tag{8.15}$$

with rotational quantum number $J = 0, 1, 2, \ldots$. Often the rotational energy levels are written as

with B defined as the rotational constant,

$$B = \frac{\hbar^2}{2I}. \tag{8.17}$$

If we were to solve equation [8.14], we would find the degeneracy g, the number of states with the same energy but different quantum numbers,

$$g_J = 2J + 1. \tag{8.18}$$

The rotational energy levels have spacing that increases with J. Interestingly, the energy transitions are constant in wavenumber or frequency, meaning that rotational lines are equally spaced in a wavenumber or frequency spectrum. We can see this by considering that allowed rotational transitions have $\Delta J = \pm 1$ for linear molecules (see Section 8.3.2). Then,

$$\Delta E = E_J - E_{J-1} = 2BJ. \tag{8.19}$$

We can use equation [8.15] to determine the order-of-magnitude energy of pure rotational spectra of diatomic molecules. Let us use the diatomic molecule CO as an example. To first order, the C and O atoms have similar atomic masses, $m_1 \sim m_2 \approx 12$ amu, and the internuclear separation in diatomic molecules is about $r_1 \sim r_2 \approx 1$ Å. We find that $E_J \sim 1.4 \times 10^{-23}$ J. This corresponds to energies at microwave frequencies: a frequency of 2×10^{10} s^{-1}, a wavenumber of 0.7 cm^{-1}, or a wavelength of 0.014 m. A pure rotational spectrum can exist at these very low energies—energies too low to excite vibrational modes of the molecule.

A complication to the rigid rotor approximation for linear diatomic molecules is that molecules are not completely rigid. The centrifugal force means that the atomic nuclei will respond to increasing rotational energy by moving further apart. The resulting increase in internuclear separation with increasing rotational quantum number J decreases the rotational energy level separation. To account for this centrifugal elongation, an extra term must be added to the rotational energy level equation. The centrifugal distortion is significant typically only for very highly rotationally excited states.

We developed the rigid rotor framework for linear diatomic molecules. The discussion is also valid for spherical tops (or any rigidly rotating dipole). For molecules that are asymmetric tops, an additional term is required.

In this section, we have not solved the Schrodinger equation, but rather asserted a solution. To gain a deeper understanding, one could follow a general approach taken in mathematical physics by formulating a guess at a solution based on solutions of similar equations. For a much more detailed derivation of molecular energy levels, there are many textbooks [e.g., 3, 4] and reference books [e.g., 5] to name a few. We will now continue on to molecular vibrational energy levels, using the same classical analogy approach we took for the rotational energy levels.

8.2.2.2 *Molecular Vibrational Transitions*

Molecules vibrate when the atoms in a molecule are in periodic motion with respect to the molecule's center of mass (Figure 8.5). Molecular vibrational transitions never occur on their own; as the molecule vibrates, the lower-energy rotational

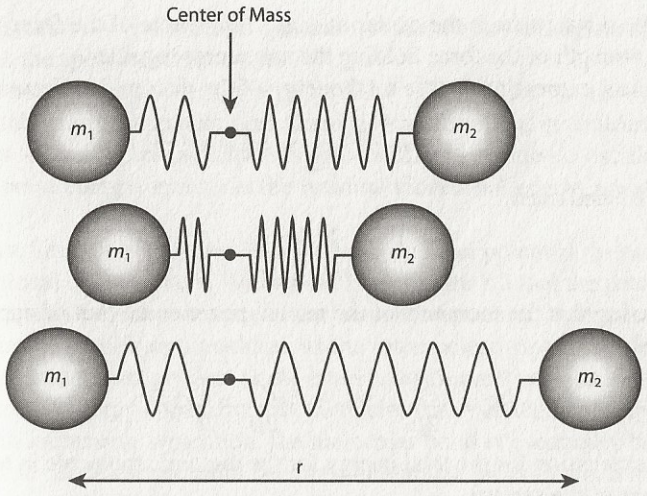

Figure 8.5 Schematic illustration of molecular vibration for a linear diatomic molecule. The simple harmonic oscillator is used as an approximate model for a diatomic molecule.

modes are also excited. Nevertheless, because the energy of the vibrational transition is much larger than that of the rotational transition, the vibrational energy levels and transitions can be considered independently of rotation to a good approximation. The so-called rotational-vibrational spectrum is an array of rotational lines grouped around a vibrational transition (Section 8.2.3).

To develop a conceptual understanding of vibrational energy levels, we will follow the discussion for rotational energy levels, again using a classical mechanics analogy limited to linear diatomic molecules. The classical analogy for diatomic molecular vibration is that of a simple harmonic oscillator. With this analogy we are limiting our attention to vibration along the axis joining the nuclei (and, again, ignoring rotational motion).

From Figure 8.3, we can see that the potential energy of a stable electronic state as a function of internuclear distance x can be approximated by a parabola. The parabola with the equilibrium point at the minimum of the potential energy means that as the atoms are displaced there is a restoring force pushing the atoms back to the equilibrium position. For a separation smaller than the equilibrium one, a strong repulsion develops. For separations greater than the equilibrium separation, the force becomes attractive. This is why the nuclei of the two atoms are essentially maintained at a more or less well-defined equilibrium separation. The approximate potential energy curve can be described by the potential energy for a simple harmonic oscillator,

$$V(x) = \frac{1}{2}Cx^2, \tag{8.20}$$

Here x is the distance from the center of mass. The value of the force constant C reflects the strength of the force holding the two atoms together.

The classical expression for the total energy of the diatomic molecule is

$$E_{\mathrm{v}} = \frac{1}{2}m_1 v_1^2 + \frac{1}{2}m_1 v_2^2 + V(x). \tag{8.21}$$

Using the reduced mass

$$\frac{1}{\mu} = \frac{1}{m_1} + \frac{1}{m_2} \tag{8.22}$$

and considering that the momenta of the nuclei, p, are equal (but of opposite magnitude), we have

$$E_{\mathrm{v}} = \frac{p^2}{2\mu} + V(x) = \frac{p^2}{2\mu} + \frac{1}{2}Cx^2. \tag{8.23}$$

This is the expression for the total energy for the diatomic molecule in terms of the reduced mass of the system,

We now associate the expression for the total energy with the quantum mechanical operator, $H\psi = E\psi$,

$$-\frac{\hbar^2}{2\mu}\frac{d^2\psi}{dx^2} + \frac{1}{2}Cx^2\psi = E_{\mathrm{v}}\psi. \tag{8.24}$$

The eigenvalue, or quantized energy level, solution to this equation is

$$E_{\mathrm{v}} = (\mathrm{v} + 1/2)h\left[\frac{1}{2\pi}\sqrt{\frac{C}{\mu}}\right], \tag{8.25}$$

which can also be written

$$\boxed{E_{\mathrm{v}_k} = h\nu_0(\mathrm{v}_k + 1/2) \quad (\mathrm{v}_k = 0, 1, 2, \ldots),} \tag{8.26}$$

where we have associated $\frac{1}{2\pi}\sqrt{C/\mu}$ with the fundamental frequency ν_0. Here v is the vibrational quantum number. The subscript k denotes the normal modes ($k = 1, 2, 3, \ldots$). There is no degeneracy in vibrational energy states, that is,

$$g_{\mathrm{v}} = 1. \tag{8.27}$$

What is so interesting about using the simple harmonic oscillator approximation is that the derived energy levels are equally spaced with a separation of $h\nu_0$. This results from a vibrational transition selection rule $\Delta\mathrm{v} = \pm 1$ (Section 8.3.3). The equal energy level separation means in principle that the energy of a vibrational transition, and hence wavenumbers and frequencies, are the same for different transitions. In practice, anharmonicity makes the energy level separations different from each other.

We can estimate the energy of vibrational transitions using the association of $\frac{1}{2\pi}\sqrt{C/\mu}$ from our simple harmonic oscillator analogy, and with knowledge of C. If we take the force constant C for the CO molecule as 1860 N m^{-2} [4], we find $\nu_0 \sim 6.4 \times 10^{13}$ Hz, corresponding to an energy of about 4×10^{-20} J, a wavelength of about 4.3 μm, and a wavenumber of about 2100 cm^{-1}, in the infrared region of the electromagnetic spectrum. More commonly, the force constant C is determined

from observations of a vibrational spectrum, rather than by taking the force constant to estimate the spectrum frequencies.

The lowest vibrational energy level is $E_0 = \frac{1}{2}h\nu_0$. That the zero-point energy is not actually zero is a quantum mechanical manifestation, in contrast to classical mechanics where the zero-point energy of a simple harmonic oscillator is zero. The zero-point energy represents the residual vibrational energy possessed by the molecule.

There are limitations to using the harmonic oscillator potential to describe molecular vibrational energy levels. We can see from Figure 8.3 that the potential energy curve for a stable electronic state is not actually a perfectly symmetric parabola. Away from the equilibrium position, as the internuclear separation decreases, the potential rises more steeply than as the internuclear separation increases. This sharp rise in potential energy comes from the repulsive forces as the nuclei approach each other. With increasing separation, the molecular bond is eventually broken. Thus the harmonic oscillator potential becomes unrealistic for both small and larger internuclear separations.

8.3.3 The Rotational-Vibrational Spectrum

The rotational-vibrational spectrum for a given vibrational transition $\Delta\mathrm{v}$ is divided into three "branches," the P-branch, Q-branch, and R-branch. These branches arise from the radiation selection rule that in a rotational transition $\Delta J = \pm 1$. The P-branch corresponds to $\Delta J = -1$ and the R-branch to $\Delta J = +1$. The Q branch corresponds to no rotational transition. For diatomic molecules there are no transitions, resulting in a "gap" in the actual spectrum. See Figure 8.6. For an example, absorption cross-sections for the linear molecule CO are shown in Figure 8.7.

Molecules have specific vibrational modes, each with a fundamental frequency with its own set of quantum numbers. These are known as normal modes or fundamental vibrational modes. Each normal mode of vibration is independent of the others and corresponds to simultaneous vibrations of different parts of the molecule. A linear molecule has only one fundamental vibrational mode, that is, only way that the molecule can vibrate (Figure 8.5). For linear molecules with more than two atoms, the number of normal modes of vibration is $3N - 5$, where N is the number of atoms and 5 is the degrees of freedom. For nonlinear molecules the number of normal modes of vibration is $3N - 6$. Figure 8.8 illustrates the different normal modes for a polyatomic linear molecule (CO_2) and a triatomic nonlinear molecule (H_2O).

In addition to the fundamental normal modes, molecules can have vibrational overtones. The first vibrational overtone would be $\mathrm{v} \rightarrow \mathrm{v} - 2$, the second vibrational overtone would be $\mathrm{v} \rightarrow \mathrm{v} - 3$, and so on. In the simple harmonic oscillator treatment of molecules, we have assumed that normal modes are fully independent. In reality, the normal modes can be coupled, giving rise to vibrations with combinations of the fundamental vibration frequencies, called combination bands.

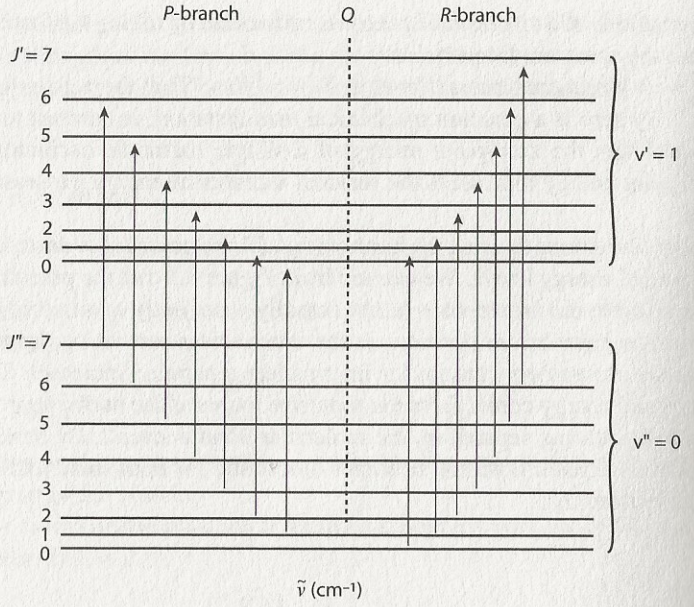

Figure 8.6 Simultaneous rotational vibrational transitions. $\Delta J = -1$ produces the P-branch, $\Delta J = -1$ produces the R-branch. For nonlinear molecules $\Delta J = 0$ produces the Q-branch.

8.2.3.1 *Molecular Electronic Transitions*

Molecules have electronic transitions that occur at much higher energy levels than vibrational or rotational transitions. We can see this by first considering how much less massive electrons are than the nuclei in the molecules, about a factor of 10^{-4} to 10^{-5}. By the Heisenberg uncertainty principle, the electrons travel much faster and must therefore have much higher energies than the rotational or vibrational motions of the nuclei. Due to this great energy difference, electronic transitions can be described independently of the rotational and vibrational transitions. The separation of electronic and nuclear motions is known as the Born-Oppenheimer approximation.

We can estimate the energy of electronic transitions by taking the momentum of an electron to be $\sim \hbar/a$, where $a \sim 1$ Å is a typical molecular size. Together with $E = p^2/m$ we have

$$E_{\rm E} \sim \frac{\hbar^2}{ma^2}. \tag{8.28}$$

The molecular electronic energy is a few eV (about a few $\times 10^{-19}$ J) or higher, which corresponds to photons at visible wavelengths or shorter.

Molecular electronic energy levels, like all atomic and molecular energy levels are quantized. Unlike for rotational and vibrational transitions, the electronic energy levels and transitions are too complex for us to present even a simple overview here. (See references listed at the end of this chapter for more information.) Elec-

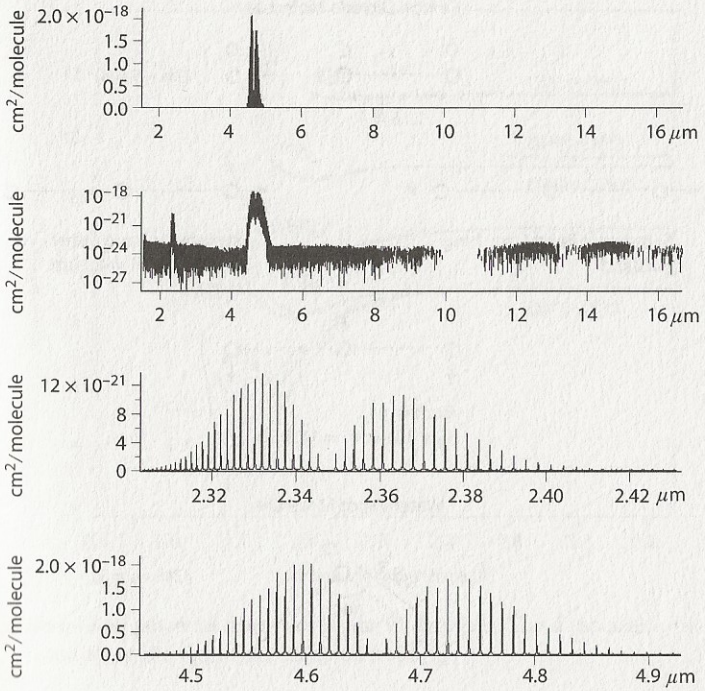

Figure 8.7 Simulated intensity of rotational-vibrational transitions of the CO molecule. The rotational transitions are centered around the P- and R-branches. The line intensities are approximately correct for a temperature of 300 K. The vibrational transition is the v = 1 − 0 band. Adapted from [6].

tronic transitions can excite molecular vibrational and rotational transitions, resulting in an electronic band with finer structure from rotational and vibrational transitions.

It can be useful to have a handle on molecular notation. For linear molecules electronic states are designated by

$$^{(2S+1)}\Lambda^{(\pm)}_{(u,g)}, \tag{8.29}$$

where S is the electron spin quantum number, $(2S+1)$ is the degeneracy, (u, g) refers to odd or even wavefunction, and $\pm$ refers to the reflection symmetry of the wavefunction. The symbol Λ refers to the orbital wavefunction type (shape), and the first three levels are denoted as Σ, Π, Δ. An example of electronic energy levels and notation is given in Figure 8.9.

8.2.4 Energy Level Populations

We now turn from energy levels and their spacing to the number density of molecules in a given excited state, n_i, where i denotes an excited state. Often referred to as the energy level populations, or sometimes occupation numbers, the

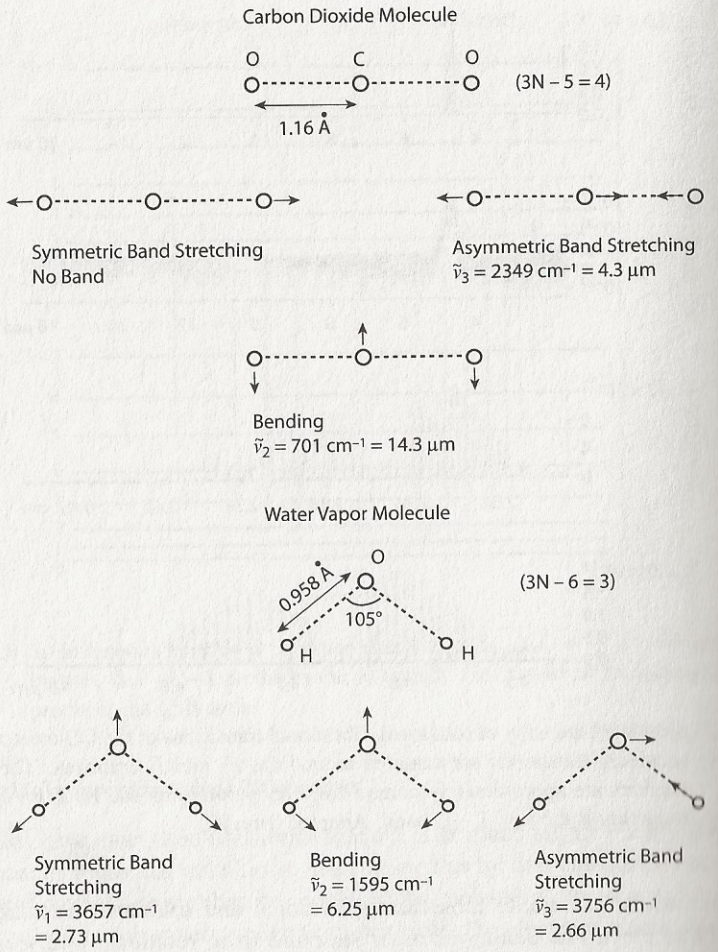

Figure 8.8 Schematic of molecular vibrational normal modes. The normal modes are independent of each other, corresponding to simultaneous vibrations of different parts of the molecule.

n_i are a basic component of the absorption coefficient (equation [8.1]). Under conditions of local thermodynamic equilibrium (LTE), we can prescribe a relatively simple formulation for the energy level populations. The formulation is simple because it depends only on temperature and not on the radiation field.

LTE is a local version of complete thermodynamic equilibrium. LTE is an approximation, whereby all precepts of thermodynamic equilibrium are assumed to hold, except that the radiation field departs from its Planckian value. LTE is a reasonable approximation valid in a local area of the atmosphere where any temperature, pressure, or chemical gradients are small compared to the photon mean free path. If collisions dominate, LTE implies a strict coupling of the matter component to the local radiation temperature, and can be used for regions of planetary

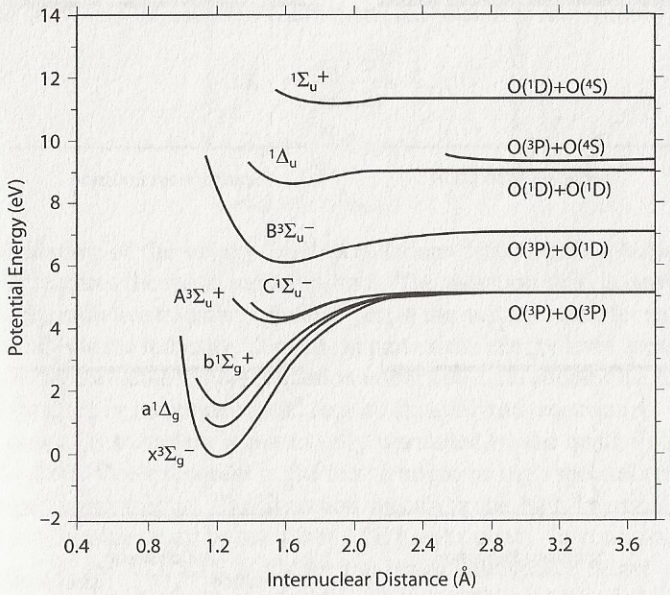

Figure 8.9 Simplified potential energy diagram for oxygen. The dissociation products are listed along the right side. Adapted from [7].

atmospheres where collisional processes dominate over radiative processes (see Figure 8.10). See Section 5.4 for an introduction to LTE and its major simplification to the radiative transfer problem.

Under LTE, the energy level populations for electronic, rotational, and vibrational states are determined by Boltzmann statistics. Hence the major simplication: energy level populations can be described by the Boltzmann formula

$$\frac{n_j}{n} = \frac{g_j e^{-E_j/kT}}{\sum_i g_i e^{-E_i/kT}}, \tag{8.30}$$

where $Q = \sum_i g_i e^{E_i/kT}$ is the partition function. Here n is the total number density of a given molecule, n_j is the number density of the molecule with energy level j, E_j is the energy of level j from the ground state, k is Boltzmann's constant, and T is the temperature. Here g is the statistical weight of the level, also known as the energy degeneracy of the level. g is an integer. The degeneracy refers to the number of distinct states having the same energy E_j but with a different set of quantum numbers.

The Boltzmann distribution for molecular rotational states is

$$\frac{n_J}{n_0} = (2J+1)e^{-BJ(J+1)/kT}, \tag{8.31}$$

where the values for g and E are from Section 8.2.2.1, and the subscript 0 refers to the ground state. For molecular vibrational states,

$$\frac{n_v}{n_0} = e^{-vh\nu_0/kT}, \tag{8.32}$$

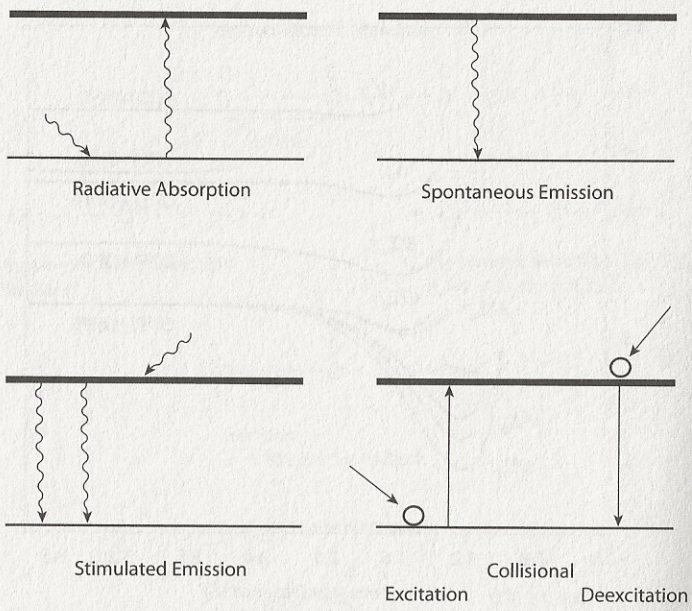

Figure 8.10 Illustration of different radiative and collisional processes for transitions between excited states, using a two-level atom for illustration. The wavy line indicates a photon. The circles represent atoms and the straight line indicates a collision. Collisions couple the matter and radiation temperature. Adapted from [8].

where the values for g and E are from Section 8.2.2.2. For a discussion of atomic energy level LTE distributions, see, for example, [9].

In planetary atmospheres LTE is valid where collisions couple the matter and radiation temperatures. In planetary atmospheres, LTE breaks down where collisions become less important than radiative transitions. One such case is at low pressures (low densities) where radiative processes dominate the competing collisional excitation processes (see Figure 8.10).

In the non-LTE case, how can the energy level populations be calculated? The answer is by use of the statistical equilibrium equations of detailed balance together with the radiation field. In detailed balance, every transition happens in both directions. In the case where radiative transitions dominate over collisional transitions, the equation of detailed balance is

$$n_u A_{ul} - n_u B_{ul} \overline{J}_\nu = n_l B_{lu} \overline{J}_\nu, \tag{8.33}$$

where the subscripts u and l refer to the upper and lower transitions, respectively. The variable $\overline{J}_\nu = \int_0^\infty J(\tau, \nu)\phi(\nu - \nu_0)d\nu$ is the mean radiation field over the transition.

The Einstein A and B coefficients in the above equation are as follows. A_{ul} in units of s^{-1} is the Einstein coefficient of spontaneous emission, B_{lu} in units of m^3 J^{-1} s^{-2} is the Einstein coefficient of induced absorption, and B_{ul} also in units of m^3 J^{-1} s^{-2} is the Einstein coefficient of stimulated emission. We leave it as an

exercise to show that the Einstein coefficients are related to each other by

$$\begin{aligned} B_{ul} &= \frac{g_u}{g_l}\frac{c^2}{2h\nu^3}A_{ul}, \\ B_{ul} &= \frac{g_l}{g_u}B_{lu}, \\ A_{ul} &= -A_{lu}. \end{aligned} \tag{8.34}$$

The calculation of the energy level populations from detailed balance (equation [8.33]) requires the mean radiation field. The radiation field is derived from a solution to the radiative transfer equation. Yet, in the radiative transfer equation, the radiation field (via the intensity) depends in part on the energy level populations. In a solution of the radiative transfer equation under non-LTE conditions, each energy level of each atom or molecule would require an additional equation.

So far, non-LTE treatment is not usually warranted by the quality of exoplanet atmosphere data. One exception in the future might be high spectral resolution of transit transmission spectra. Transmission spectra probe high layers of the atmosphere where densities may be such that LTE breaks down. In contrast, in Earth's atmosphere (Figure 9.2), LTE holds for the lower atmosphere below altitudes of about 60–70 km. A thorough description of non-LTE conditions of validity and treatment can be found in [9, 10].

8.3 MOLECULAR ABSORPTION CROSS SECTIONS

We now move on to the absorption cross section $\sigma_{lu}(\nu)$ or $\sigma_{lu}(\tilde{\nu})$ for a molecular rotational or vibrational energy transition. The absorption cross section is made up of two components, the strength of the transition itself and a line broadening function. Molecular lines are never truly monochromatic, but due to a variety of physical processes are spread out in frequency. We therefore define the cross section in terms of the transition line strength S_{lu} and the normalized line broadening function $f(\tilde{\nu} - \tilde{\nu}_0)$,

$$\sigma_{lu} = S_{lu} f(\tilde{\nu} - \tilde{\nu}_0). \tag{8.35}$$

S is more formally called the spectral line intensity in units of $cm^{-1}/(molecule\ cm^{-2})$ and $\tilde{\nu}_0$ is the wavenumber of a monochromatic line. f is normalized as

$$\int_{-\infty}^{\infty} f(\tilde{\nu} - \tilde{\nu}_0)d\tilde{\nu} = 1. \tag{8.36}$$

We may also write

$$\int_{-\infty}^{\infty} \sigma_{lu}(\tilde{\nu})d\tilde{\nu} = S_{lu}, \tag{8.37}$$

again stating that the absorption coefficient is not delta-function-like at a monochromatic frequency, but has a spread in frequency owing to line broadening mechanisms.

8.3.1 Line Strengths

Let us treat the line strength by first relating it to the Einstein coefficients. We have the definition (equation [8.35])

$$\alpha_l = n_l \sigma_{lu} = n_l S_{lu} f(\tilde{\nu} - \tilde{\nu_0}). \tag{8.38}$$

But we could also show that the energy removed from a beam of radiation is

$$\alpha_l = \frac{h\tilde{\nu}_0}{4\pi c} \left(n_l B_{lu} - n_u B_{ul}\right) f(\tilde{\nu} - \tilde{\nu}_0), \tag{8.39}$$

where we have treated stimulated emission as negative absorption. We can write

$$\alpha_l = n \left[\frac{h\tilde{\nu}_0}{4\pi c} \frac{n_l}{n} B_{lu} \left(1 - \mathrm{e}^{-h\tilde{\nu}_0/ckT}\right)\right] f(\tilde{\nu} - \tilde{\nu}_0), \tag{8.40}$$

where we have assumed LTE to use the Boltzmann distribution equation for energy level populations (equation [8.30]). We associate the LTE line strength with the term in square brackets,

$$S_{lu} = \left[\frac{h\tilde{\nu}_0}{4\pi c} \frac{n_l}{n} B_{lu} \left(1 - \mathrm{e}^{-h\tilde{\nu}_0/ckT}\right)\right], \tag{8.41}$$

and we have implicitly redefined $\alpha = n\sigma_{lu}$, with σ_{lu} weighted by n_l/n.

We are now left to describe where the Einstein B coefficient comes from. B_{lu} comes from quantum mechanics. Essentially,

$$B_{lu} = \frac{8\pi^3 \tilde{\nu}_0}{3hc} \left| \int \Phi_u^* (\overline{\mu} \Phi_l) dV \right|^2 \left| \int \Sigma_u^* \Sigma_l d\sigma \right|^2. \tag{8.42}$$

Here $\Phi(r, \theta, \phi)$ is the space-dependent part of the wavefunction, $\Sigma(\sigma)$ is the spin-dependent part of the wavefunction, and $\overline{\mu}$ is the dipole moment operator. From all of the above, if we were able to carry out detailed quantum mechanical calculations, we could compute the spectral line intensity of a given molecular transition.

The theoretical computation or laboratory measurement of lines and line transition identification is a whole research field of its own. In exoplanet atmospheres research we typically take the line strength directly from a molecular database, such as HITRAN [11]. In the HITRAN database, the line strength at STP is given, and one may scale it according to

$$\boxed{S_{lu}(T) = S_{lu}(T_{\mathrm{ref}}) \frac{Q(T_{\mathrm{ref}})}{Q(T)} \frac{\exp(-c_2 E_l/T)}{\exp(-c_2 E_l/T_{\mathrm{ref}})} \frac{\left[1 - \exp(-c_2 \tilde{\nu}_{lu}/T)\right]}{\left[1 - \exp(-c_2 \tilde{\nu}_{lu}/T_{\mathrm{ref}})\right]}} \tag{8.43}$$

Here E_l is the lower state energy in cm^{-1}, c_2 is the second radiation constant hc/k = 1.4388 cm K, and $\tilde{\nu}$ is still the wavenumber in cm^{-1}. The second term on the right-hand side accounts for a temperature scaling of the partition function, the third term for the ratio of the Boltzmann populations, and the fourth term for stimulated emission.

8.3.2 Selection Rules for Molecules

Out of all the existing energy levels of a given molecule (including electronic, rotational, and/or vibrational energy levels), transitions happen only between some of the energy levels. The allowed transitions are described by "selection rules."

A selection rule is a quantum mechanical rule describing transitions that are permitted. The transition selection rules ultimately come from equation [8.42], from a quantum mechanical description of the eigenfunction or the wavefunctions of each of the two energy levels involved in a given energy transition. Where equation [8.42] vanishes, there is no transition. Where $B_{lu} \gg 0$, the transition is "permitted," and where B_{lu} is very small, the transition is "forbidden." A forbidden transition is forbidden to "first order" only; they are rare and hence weak. We can think of forbidden as meaning unfavorable.

For example, if there is no dipole moment, equation [8.42] goes to zero. This is a more formal basis for our earlier conceptual remarks that a molecule must posses a dipole moment in order to interact with electromagnetic radiation to produce a rotational or rotational-vibrational spectrum.

As a second example, $\Phi_u^*(\overline{\mu}\Phi_l)$ must be an even function to prevent significant cancellation between volume elements. Since $\overline{\mu}$ is an odd function in space, then Φ_u^* and Φ_l must have opposite parity. This formally leads to the rotational and vibrational energy transition selection rules as follows. For rotational energy transitions in a linear molecule $\Delta J = \pm 1$. Additionally, for a nondiatomic simultaneous rotational-vibrational transition where the vibration is perpendicular to the rotational axis, $\Delta J = 0, \pm 1$. For vibrational transitions in all molecules, $\Delta \mathrm{v} = \pm 1$. This means in principle that, for polyatomic molecules, overtones (e.g., $\mathrm{v} = 0 \rightarrow \mathrm{v} = 2$) are not allowed, nor are combination bands (e.g., transitions in two normal modes at the same time). In reality, the selection rules can be violated if perturbations affect the symmetry of the wavefunctions, namely, overtone and combination bands are observed.

8.3.3 Line Broadening

We have one remaining ingredient to describe for the absorption cross section and that is line broadening. Molecular energy transitions are not precise, that is, they do not absorb or emit photons that are monochromatic. Monochromatic emission is practically never observed. Energy levels during energy transitions are always slightly altered for an individual molecule, by both internal and external influences. These changes in energy cause spectral lines to have finite widths in frequency.

8.3.3.1 Natural Broadening

Natural broadening is line broadening caused by the uncertainty in the values of energy levels. If the energy levels are not precisely known, the energy and hence frequency of an emergent photon will be different at different times. Even though

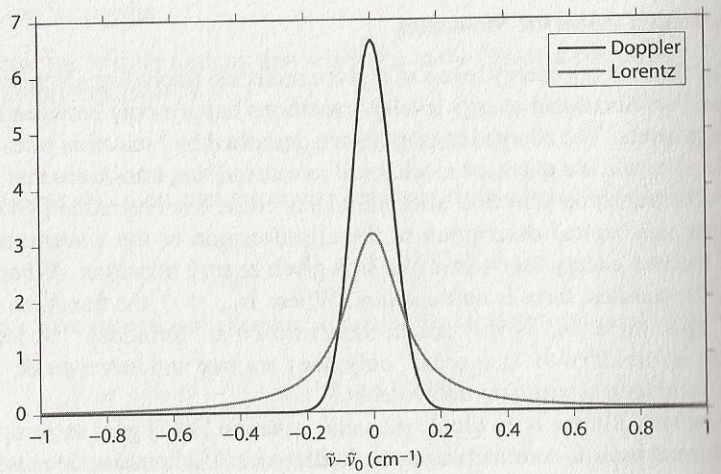

Figure 8.11 Comparison of Doppler and collisional broadening. The y-axis is the normalized probability density.

natural broadening is negligible in planetary atmospheres we describe it here for completeness.

Natural broadening comes from the Heisenberg uncertainty principle, that time and energy cannot both be precisely known,

$$\Delta E \Delta t = \frac{h}{2\pi} \tag{8.44}$$

or

$$\Delta \nu \Delta t = \frac{1}{2\pi}. \tag{8.45}$$

We may then write the line broadening in frequency as

$$\Delta \nu = \frac{1}{2\pi \Delta t} = 2A_{ul}, \tag{8.46}$$

where A_{ul} is the Einstein A coefficient described in equation [8.34].

Natural broadening is described by the Lorentz profile

$$f_{\mathrm{N}}(\nu - \nu_0) = \frac{1}{\pi} \frac{\gamma_{\mathrm{N}}}{(\nu - \nu_0)^2 + \gamma^2}, \tag{8.47}$$

where γ_{N} is the full-width at half maximum (FWHM), $\gamma \simeq 1/2\pi t$, where t is the radiative lifetime. Note that α is often used instead of γ; here we are trying to avoid confusion with the absorption coefficient α.

8.3.3.2 *Doppler Broadening*

Doppler broadening arises from the difference in thermal velocities of atoms and molecules. Recall the Doppler shift

$$\nu = \nu_0 \left(1 \pm \frac{v}{c}\right), \tag{8.48}$$

where ν is the frequency, ν_0 is the rest frequency, v is the velocity, and c is the speed of light.

There is a distribution of speeds along the line of sight which creates line broadening. We will assume that the distribution of speeds is given by the Maxwell-Boltzmann distribution

$$P(v)dv = \sqrt{\frac{m}{2\pi kT}} \exp\left(\frac{-mv^2}{2kT}\right) dv, \tag{8.49}$$

where $P(v)dv$ is the fraction of particles with speeds v along the line of sight.

We can substitute the Doppler shift (equation [8.48]) into the Maxwell-Boltzmann distribution to find an expression for Doppler line broadening,

$$\boxed{f_{\mathrm{D}}(\nu - \nu_0) = \frac{1}{\gamma_{\mathrm{D}}\sqrt{(\pi)}} \exp\left[-\left(\frac{\nu - \nu_0}{\gamma_{\mathrm{D}}}\right)\right],} \tag{8.50}$$

where

$$\gamma_{\mathrm{D}} = \nu_0 \sqrt{\frac{2kT}{mc^2}}. \tag{8.51}$$

Because the Doppler broadening equation is a Gaussian, γ_{D} is the standard deviation. The FWHM of the Doppler-broadened line is

$$\mathrm{FWHM} = \gamma_{\mathrm{D}} \sqrt{\ln 2}. \tag{8.52}$$

We can see from the exponential term in the Doppler broadening equation (equation [8.50]) that the spectral line will be more intense at line center and weaker in the line wings (see Figure 8.11). From the Doppler broadening equation we can also see how the line broadening depends on temperature.

8.3.3.3 *Collisional Broadening*

Collisional, or pressure, broadening describes line broadening due to collisions between atoms and molecules. If we take atomic and molecular collisions to be instantaneous, the principal effect of the collision is to destroy the phase coherence of the emitted wave train. In other words, after the collision, the molecule starts emitting at another phase; new phases are randomly distributed. This random distribution of phases together with the Poisson distribution for collisions leads to the Lorentz profile

$$\boxed{f_{\mathrm{L}}(\nu - \nu_0) = \frac{1}{\pi} \frac{\gamma}{(\nu - \nu_0)^2 + \gamma^2}.} \tag{8.53}$$

Here ν_0 is the frequency of an ideal monochromatic line, and γ is the half width of the line at half maximum. ν and ν_0 may be defined as wavenumber as long as γ is also defined in the same units. For a derivation of the Lorentz profile for both collisional broadening and natural line broadening, see [7,8].

The parameter γ is complicated to calculate, and comes from quantum mechanics calculations or from laboratory measurements. Based on the kinetic theory of gases, however, we may scale γ as

$$\gamma = \gamma_0 \frac{P}{P_0} \left(\frac{T_0}{T} \right)^n, \tag{8.54}$$

where the subscript 0 refers to standard temperature ($T_0 = 273$ K) and pressure ($P_0 = 1013$ mbar). The broadening exponent n has a classical value that is 0.5, whereas real molecular lines have broadening exponents ranging from about 0.4 to 0.75. In the above equation, increased pressure can be understood as increasing the concentration of molecules available for collisions, and hence increasing γ. We can think of an increase in temperature as an increase in velocity whereby the molecules spend less time perturbing each other because they are in each other's vicinity for a shorter time. Finally, if an approximate value of the collisional broadening parameter is warranted, the van der Waals collisional broadening theory can be used to estimate γ [e.g., 9].

8.3.3.4 Combined Doppler and Lorentz Line Broadening

What is the form of a combined Doppler and Lorentz broadening profile? To account for all possible thermal velocities, a convolution of the two line shapes is needed,

$$f_{\rm Voigt}(\nu - \nu_0) = \int_{-\infty}^{\infty} f_{\rm L}(\nu' - \nu_0) f_{\rm D}(\nu - \nu') d\nu'. \tag{8.55}$$

Substituting the Lorentz and Doppler broadening terms we have

$$f_{\rm Voigt}(\nu - \nu_0) = \frac{1}{\pi^{3/2}} \frac{\gamma}{\gamma_{\rm D}} \int_{-\infty}^{\infty} \frac{1}{(\nu' - \nu_0)^2 + \gamma^2} \exp\left[-\frac{(\nu - \nu')^2}{\gamma_{\rm D}^2} \right] d\nu'. \tag{8.56}$$

We can simplify the above expression by defining

$$t \equiv \frac{(\nu - \nu')}{\gamma_{\rm D}}; \quad y \equiv \frac{\gamma}{\gamma_{\rm D}}; \quad x \equiv \frac{(\nu - \nu_0)}{\gamma_{\rm D}}. \tag{8.57}$$

We then find

$$\boxed{f_{\rm Voigt}(\nu - \nu_0) = \frac{1}{\gamma_{\rm D}\sqrt{\pi}} K(x, y),} \tag{8.58}$$

where

$$K(x, y) = \frac{y}{\pi} \int_{-\infty}^{\infty} \frac{1}{y^2 + (x - t)^2 \exp(-t^2)} dt. \tag{8.59}$$

8.4 RAYLEIGH SCATTERING

Rayleigh scattering is the dominant opacity at short wavelengths and because of its λ^{-4} dependence is responsible for Earth's blue sky (see Figures 1.2 and 6.11).

Rayleigh scattering is derived and described in detail in many textbooks, e.g., [10]. Here we simply provide formulae for completeness. Rayleigh scattering is valid for molecules or for any particle that is much smaller than the wavelength of light.

The Rayleigh scattering cross section in m^2 is

$$\sigma_{\rm scat}(\lambda) = \alpha_{\rm p}^2 \frac{128\pi^5}{3\lambda^4}, \tag{8.60}$$

where $\alpha_{\rm p}$ is the polarizability

$$\alpha_{\rm p} = \frac{3}{4\pi n} \left(\frac{m^2 - 1}{m^2 + 2} \right), \tag{8.61}$$

where n is the number density of molecules and m is the refractive index (or a weighted average of the refractive indices). Using the definition of polarizability, and considering that $m \sim 1$, the Rayleigh scattering cross section can be written

$$\sigma_{\rm scat}(\lambda) = \frac{8\pi^3 \left(m^2 - 1\right)^2}{3\lambda^4 n^2}. \tag{8.62}$$

A useful numerical formula for the Rayleigh scattering cross section for Earth's atmosphere is

$$\sigma_{\rm scat}(\lambda) = \lambda^{-4} \sum_{i=0}^{3} a_i \lambda^{-2i} \times 10^{-28}, \tag{8.63}$$

in units of cm^2. This formula is accurate to 0.3% on the range $0.205 < \lambda < 1.05$ μm. Here the coefficients are $a_0 = 3.9729066$, $a_1 = 4.6547659$, $a_2 = 4.5055995 \times 10^{-4}$ and $a_3 = 2.3229848 \times 10^{-5}$ [12].

For H_2 a convenient formula can be found in [13],

$$\sigma_{\rm scat}(\lambda) = \frac{8.14 \times 10^{-13}}{\lambda^4} + \frac{1.28 \times 10^{-6}}{\lambda^6} + \frac{1.61}{\lambda^8}, \tag{8.64}$$

in units of $Å^2$.

8.5 CONDENSATE OPACITIES

We now turn to discuss the absorption and scattering coefficients of condensates. Condensates are solid particles, including not only liquid water droplets and water ice that make up Earth atmospheric clouds, but any cloud or haze particle that is liquid or solid. We must treat condensates separately from gas particles because as aggregrates of molecules they have no well-defined energy levels or rotational or vibrational states.

We can see many beautiful examples of scattering by condensates. Bright colorful single and double rainbows arise from refraction of sunlight through spherical water droplets. Another, more rare example is the so-called glory. The glory appears as circular colored rings inside which is the observer's shadow. The glory arises from light backscattered toward its source by water droplets of uniform size. The glory is commonly observed from airplanes or mountain tops, since the observer has to be directly between the water droplets and the Sun. The rainbow, glory, and other scattering phenomena are caused by reflection, refraction, and diffraction of light by or through particles.

8.5.1 Analytic Phase Functions

Condensate scattering is described using the single scattering phase function, because of the strong directional dependence of condensate scattering. The phase function describes the redirection in the incident intensity to the outgoing intensity and as such the 3D directional scattering probability. The phase function is described in terms of the scattering angle Θ and is normalized:

$$\frac{1}{4\pi}\int_{\Omega} P(\Theta)d\Omega = 1. \tag{8.65}$$

Θ can be expanded as

$$\begin{aligned}\cos\Theta = \Omega\cdot\Omega' &= \Omega_x\Omega'_x + \Omega_y\Omega'_y + \Omega_z\Omega'_z \\ &= \cos\theta\cos\theta' + \sin\theta\sin\theta'\cos(\phi'-\phi)\end{aligned} \tag{8.66}$$

in the Cartesian and spherical polar coordinate system described in Figure 2.4, but using θ as the angle away from the z-axis instead of ϑ. Here the prime refers to the direction of incidence and the terms with no prime refer to the direction after scattering. The term forward scattering is used for $\Theta < \pi/2$ and backward scattering for $\Theta > \pi/2$.

Some analytic examples of the phase function include isotropic scattering

$$P(\Theta) = 1; \tag{8.67}$$

Rayleigh scattering

$$P(\Theta) = \frac{3}{4}(1+\cos^2\Theta); \tag{8.68}$$

and the Henyey-Greenstein phase function

$$P(\Theta) = \frac{1-g^2}{(1+g^2-2g\cos\Theta)^{3/2}}. \tag{8.69}$$

The Henyey-Greenstein phase function is a one-parameter fit to an actual phase function, but actually has no physical basis. The variable g is the anisotropy parameter, $-1 \le g \le 1$, and $g = 0$ for isotropic scattering or symmetric scattering.

$$g = \langle\cos\Theta\rangle = \frac{1}{4\pi}\int_{\Omega}\cos\Theta P(\Theta)d\Omega. \tag{8.70}$$

The Henyey-Greenstein phase function has been widely used because of its simplicity and convenient form for numerical simulations. Other phase functions can be described by an expansion in terms of the Legendre polynomials (see, e.g., [8, 10]). For many cases of condensate scattering, there is no analytic form, and we resort to tables generated by geometric optics or by Mie theory.

8.5.2 Description of Phase Functions from Geometric Optics

Geometric optics provides us with a conceptual description of phase function features. The geometric optics approximation to light scattering is valid when the scattering particle is very large compared to the wavelength of light. By considering a number of uniformly spaced rays striking a particle (Figure 8.12), taking

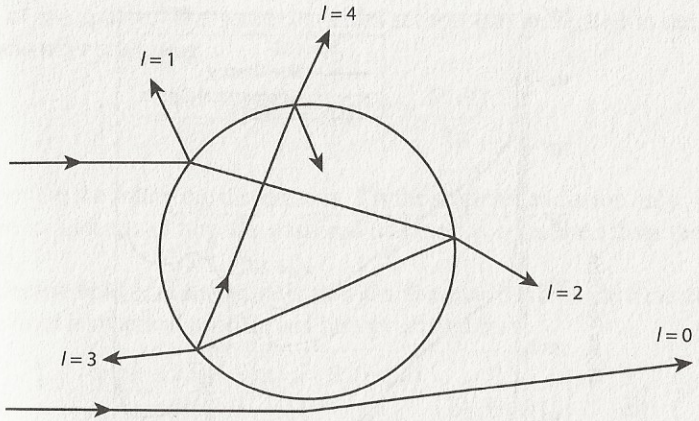

Figure 8.12 Paths of light rays reflected, refracted, or diffracted by a sphere. $l = 0$ shows a diffracted ray, $l = 2$ shows a twice refracted ray, $l = 3$ shows a ray with one internal reflection, and $l = 4$ shows a ray with two internal reflections. Adapted from [14].

into account reflection, transmission, and refraction, and summing the results over all incident rays and all significant components ($l = 0, 1, 2, \ldots$), one can derive a phase function like that shown in Figure 8.13.

Following [14] we will describe the phase function features using the indices of refraction of liquid water. Let us go through some of the phase function features in Figure 8.13, which compares results from geometric optics to Mie theory for different sized particles. All of the phase functions in Figure 8.13 notably show very similar features. At zero degrees, in the forward scattering direction, there is a very strong feature due to diffraction. We can see that diffraction increases as the particle size increases compared to the wavelength of light. The next notable features are at 137° and 130°. These features are the primary and secondary rainbows, related to rays with $l \ge 3$. At the backscattering angle (near 180°) there is a huge effect for large particles—this is the glory. The glory feature is not due to reflected rays ($l = 0$) but to surface waves on the sphere originating by interference. We can see from Figure 8.13 that features caused by light interference are not captured by geometric optics.

8.5.3 Mie Theory

We now turn to the Mie theory, which describes how to derive the phase functions and absorption and scattering cross sections of solid or liquid particles. Mie theory is a solution to Maxwell's equations for scattering of electromagnetic radiation of spherical particles. Mie theory is actually an analytic solution to Maxwell's equations and not a physical theory. It is fascinating that the Mie theory was developed over 100 years ago by Mie, and independently by others. In the limit $r \gg \lambda$ Mie

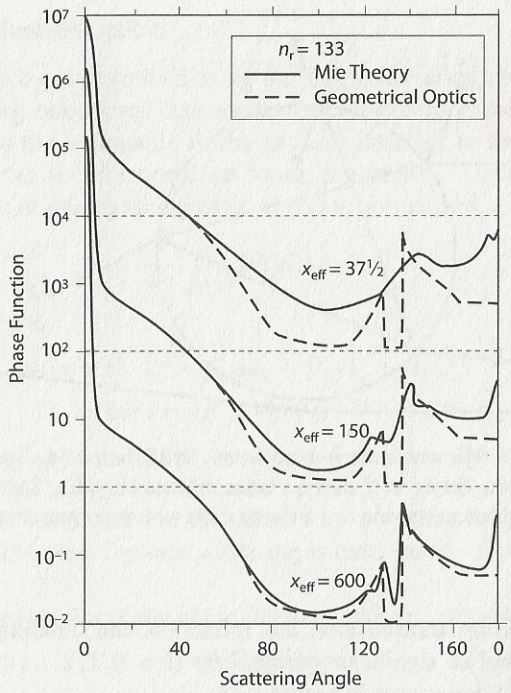

Figure 8.13 The phase function for single scattering by spherical liquid water droplets. A comparison of geometric optics and Mie theory phase functions. Mie theory captures interference between light rays whereas geometric optics does not. The phase functions for different size parameters $x = 2\pi r/\lambda$ are shown, where the subscript refers to an effective size for a particle distribution. Adapted from [14].

theory agrees with geometric optics and in the limit $r \ll \lambda$ Mie theory reduces to Rayleigh scattering. Here r is the particle radius and λ is wavelength of light as before. Mie theory is derived and applied in great detail in several excellent references [8, 10, 14–16]. Here we summarize the most important formulae, following [8, 14], to try to capture how the calculation would be carried out.

The main parameters we are interested in are those we need for the radiative transfer equation. The parameters include the scattering phase function $P(\Theta)$ (from which the related scattering asymmetry factor g can be computed), the scattering cross section $\sigma_{\rm scat}$, and the absorption cross section $\sigma_{\rm abs}$. In Mie theory the absorption and scattering cross sections are written in terms of the scattering and absorption effienciencies $Q_{\rm scat}$ and $Q_{\rm abs}$, $Q_{\rm scat} = \frac{\sigma_{\rm scat}}{\pi r^2}$ where r is the particle radius.

To get a handle on the origin of the above parameters of interest, we must take the definition of a scattering cross section as the amount of energy removed from the direction of incidence due to a single scattering event. The scatterer is the center of a sphere with radius R whereby the energy is redistributed isotropically on the

surface of the sphere. The scattering cross section can be related to the intensity before and after scattering

$$I(\Theta) = I(0)\frac{\sigma_{\rm scat}}{R^2}\frac{P(\Theta)}{4\pi} \tag{8.71}$$

Here and in the following discussions, I is the scattered radiation only. We therefore need to understand how the scattered radiation is calculated from the incident radiation.

The electric field of scattered radiation at a distance R (in the far field defined by $R \gg \lambda$) from a spherical particle can be represented by

$$\left\{ \begin{array}{c} E^s_\perp \\ E^s_\parallel \end{array} \right\} = \frac{\exp(-ikR + ikz)}{ikR} \left\{ \begin{array}{cc} S_1(\Theta,\phi) & 0 \\ 0 & S_2(\Theta,\phi) \end{array} \right\} \left\{ \begin{array}{c} E^i_\perp \\ E^i_\parallel \end{array} \right\}. \tag{8.72}$$

Here Θ is the scattering angle, and ϕ is an azimuthal angle measured about the direction of scatter. The incident radiation is propagating in the z-direction. For nonspherical particles, the above 2×2 scattering matrix is full. Here $E_\perp$ and $E_\parallel$ are the components perpendicular and parallel to the plane of scattering, where the plane of scattering is defined as the plane containing the directions of incidence and scattering. The superscripts i and s refer to incident and scattered, respectively. Our discussion is valid for isotropic, homogeneous spheres that scatter independently of each other (interference of light scattered by different particles is negligible).

To relate the above description of the electric field to the intensity before and after scattering we will use the definition in Section 7.2.2 and equation [7.7].

$$I = \langle E_\parallel E^*_\parallel + E_\perp E^*_\perp \rangle = \langle A^2_\parallel + A^2_\perp \rangle, \tag{8.73}$$

so that using equation [8.72], we then have

$$I = \frac{\sigma_{\rm scat}}{4\pi} P^{11} I_0, \tag{8.74}$$

where $\sigma_{\rm scat}$ is the scattering cross section and

$$\frac{\sigma_{\rm scat}}{4\pi} P^{11} = I/I_0 = \frac{1}{2}(S_1 S^*_1 + S_2 S^*_2). \tag{8.75}$$

For the other P matrix elements see [1].

Mie theory also gives the scattering and extinction cross sections as

$$\sigma_{\rm scat} = \pi r^2 \frac{2}{x^2} \sum_{n=1}^{\infty} (2n+1)(a_n a^*_n + b_n b^*_n), \tag{8.76}$$

$$\sigma_{\rm ext} = \pi r^2 \frac{2}{x^2} \sum_{n=1}^{\infty} (2n+1)\mathcal{R}(a_n + b_n), \tag{8.77}$$

where $\mathcal{R}$ denotes the real part of a_n and b_n, $\sigma_{\rm abs} = \sigma_{\rm ext} - \sigma_{\rm scat}$, and $\tilde{\omega} = \sigma_{\rm scat}/\sigma_{\rm ext}$. Here we have used the size parameter $x \equiv 2\pi r/\lambda$.

The heart of the Mie theory is the solution for the scattering amplitudes S_1 and S_2 and their parameters:

$$S_1 = \sum_{n=1}^{\infty} \frac{2n+1}{n(n+1)}[a_n \pi_n + b_n \tau_n], \tag{8.78}$$

$$S_2 = \sum_{n=1}^{\infty} \frac{2n+1}{n(n+1)}[b_n \pi_n + a_n \tau_n]. \tag{8.79}$$

The Mie theory solutions for S_1 and S_2 are properly interpreted as a multipole expansion of the scattered radiation. For example, a_1, a_2, and a_3 are the amount of electric dipole, quadrupole, and octopole radiation. The parameters b_n are similar coefficients for magnetic multipole radiation. Both a_n and b_n are generally complex. The computation of a_n and b_n is the central problem in computing the particle absorption and scattering cross sections and the phase functions. Their computation is related to spherical Bessel functions, and they can also be computed from recursion relations. From [8],

$$a_n = \frac{m\phi_n(mx)\phi_n'(x) - \phi_n(x)\phi_n'(mx)}{m\phi_n(mx)\zeta_n'(x) - \zeta_n(x)\phi_n'(mx)}, \tag{8.80}$$

$$b_n = \frac{\phi_n(mx)\phi_n'(x) - m\phi_n(x)\phi_n'(mx)}{\phi_n(mx)\zeta_n'(x) - m\zeta_n(x)\phi_n'(mx)}, \tag{8.81}$$

where $m = m_\mathrm{p}/m_\mathrm{a}$ is the ratio of the refractive indices of the particle (p) and the surrounding atmosphere (a). The index of refraction is complex, $m_\mathrm{p} = n_{\mathrm{p},r} + in_{\mathrm{p},i}$ where r refers to the real part of the refractive index and i to the complex part. The Ricatti-Bessel functions are ϕ and ζ, with primes denoting differentiation with respect to x or mx.

The parameters π and τ are functions only of the scattering angle Θ, are related to the Legendre polynomials, and are computed from recursion relations:

$$\pi_n(\Theta) = \frac{P_n^1(\Theta)}{\sin\Theta}, \tag{8.82}$$

$$\tau_n(\Theta) = \frac{dP_n^1(\Theta)}{d\Theta}, \tag{8.83}$$

where P_n is the associated Legendre polynomial. The first few terms are $\pi_1(\Theta) = 1, \pi_2(\Theta) = 3\cos(\Theta), \tau_1(\Theta) = \cos(\Theta), \tau_2(\Theta) = 3\cos 2\Theta$.

We now finish the Mie theory section with a general discussion of significant points to take away. We emphasize that the expressions for a_n and b_n are related only to the index of refraction and the size parameter $x \equiv 2\pi r/\lambda$, where again r is the particle radius and λ is the wavelength of light. In addition, the π_n and τ_n are functions only of the scattering angle Θ.

The solutions to S_1 and S_2 are infinite series. How many terms should actually be included? This depends on the size parameter x, since a_n and b_n both rapidly approach zero when $n \gg x$. The total number of terms need be only slightly larger than x.

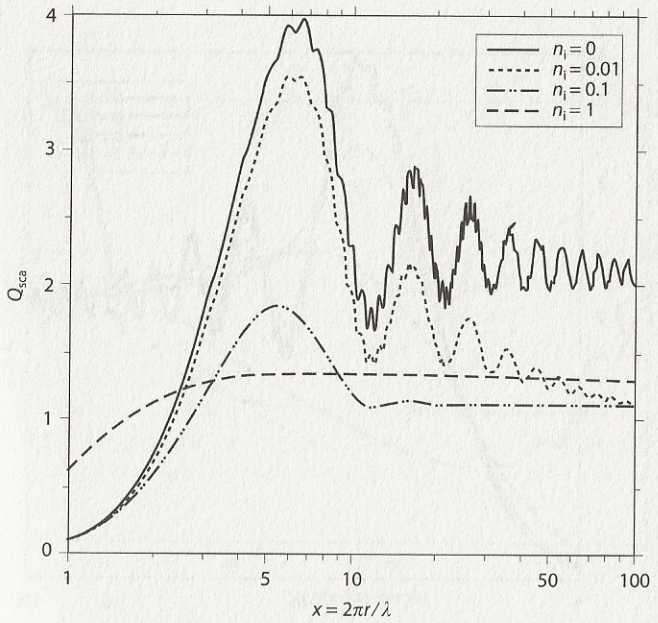

Figure 8.14 The scattering efficiency factor Q_scat as a function of the size parameter $x = 2\pi r/\lambda$. The refractive index $n_r = 1.33$ is that for liquid water. Different cases of the imaginary refractive index are shown and for decreasing values the interference effects diminish. Adapted from [14].

Mie theory is valid for spherical particles only. For nonspherical particles geometric optics approximations must be used.

Let us proceed to describe the outcomes of computations of Mie theory [14]. We will start with the scattering efficiency as a function of size parameter $x = 2\pi r/\lambda$. Figure 8.14 shows the scattering efficiency parameter $Q_\mathrm{scat} = \frac{\sigma_\mathrm{scat}}{\pi r^2}$ with a fixed real refractive index $n_r = 1.33$, but for varying complex refractive indices. Note that this is the refractive index for liquid water, and the complex part of the refractive index of water is negligible. The real part of the refractive index indicates scattering, whereas the imaginary part indicates the amount of absorption. If $n_i = 0$, the condensate particle does not absorb, it only scatters radiation. Q_scat as a function of the size parameter x shows ripples in the curve that are most prominent for $n_i = 0$. The peaks of enhanced scattering are caused by interference effects between diffracted light rays and rays that refract twice through the particle. This effect gets damped out for absorptive particles (e.g., increasing n_i). Real clouds are made of a distribution of particle sizes (see Section 4.4.4). The ripple effect also gets washed out for a dispersion of particle sizes (Figure 8.15).

Mie theory results for three different high-temperature condensates relevant for hot Jupiters are shown in Figures 8.16 and 8.17.